International Journal of Development Mathematics Vol 1 Issue 4 Page No. 152 - 165

INTERNATIONAL JOURNAL OF DEVELOPMENT MATHEMATICS

ISSN: 3026-8656 (Print) | 3026-8699 (Online)

journal homepage: https://ijdm.org.ng/index.php/Journals

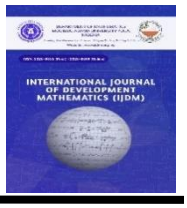

Effect of Relaxation Times on Magnetization of Blood Proton Spins at Steady State using Improved Bloch NMR Fluid Flow Equation

Rasheed A. Lateef [a*], Usman Adam[a], Timtere Pascal[a], Agada L. Emeka[b], Rilwan Salau[c]

[a]*Deartment of Physics Modibbo Adama University Yola, Adamawa State, Nigeria.*

[b]*Department of Physics Yobe State University, Damaturu, Yobe State, Nigeria.*

[c]*Department of Physics University of Maiduguri, Borno State, Nigeria.*

ARTICLE INFO

Article history:
Received 17 July 2024
Received in revised form 05 October 2024
Accepted 19 October 2024

Keywords:
Improved Bloch NMR fluid flow equation, Blood vessels, phase coherence.

MSC 2020 Subject classification:
44A10, 35M20, 34A30

ABSTRACT

Nuclear magnetic resonance (NMR) is a phenomenon that involves the absorption and re-emission of electromagnetic radiation by blood proton spins flowing through human vessels. NMR is governed by Bloch NMR fluid flow equation, which can be used to define the magnetization of blood proton spins. In the existing literature, the Bloch NMR fluid flow equation has been derived, and it has been observed that the equation does not incorporate certain NMR and blood flow parameters. In this paper, we derived a novel Bloch NMR magnetization flow equation that encompasses NMR parameters such as Larmor frequency of spinning protons and static magnetic field. We utilized the principle of dimensional homogeneity to check the validity of our newly derived NMR flow equation. Furthermore, we investigated the effect of transverse relaxation times of arterial, venous and capillary blood on magnetization of blood spinning protons. We employed Laplace transform method to obtain the steady state solution of the improved Bloch NMR fluid flow equation. MATLAB and Origin software tools were used for data analysis and simulations. Results showed that for varied transverse relaxation times of arterial, venous and capillary blood, respectively, the magnetization distribution of blood spinning protons consists of two components: the linear and the non-linear components. The findings of the study also indicated that capillary blood proton spins exhibit phase coherence. The simulated results may be used by spectroscopists to improve the accuracy of NMR/magnetic resonance imaging (MRI) experiments.

1. Introduction

Nuclear magnetic resonance (NMR) is an indispensable tool used in medicine and surgery for getting valuable information on blood flowing along human vessels (Rasheed & Usman, 2023). NMR refers to the phenomenon, in which the magnetic spin properties of the nuclei of a material, such as human blood, are excited by the application of both static magnetic field and time-varying magnetic field. This results in the creation of both spin-spin and spin-lattice magnetization within the nuclei, which can be detected and analyzed to provide information about the physical and chemical properties of the material being studied (Strogatz, 2018). NMR can be utilized in advanced medical imaging techniques such as in magnetic resonance imaging (MRI) to detect cancer and brain tumor (Gao *et al.,* 2019; Turkbey *et al*., 2011). It can be used to determine blood flow rate and other blood flow parameters such as spin-spin relaxation time, spin-lattice relaxation time, blood flow velocity and blood cross-sectional area (De, 2018; Rasheed & Usman, 2023). Nuclear magnetic resonance can be classified into two types: proton NMR and carbon NMR. Proton NMR (PNMR) is used to determine the type and number of hydrogen atoms and spatial arrangement of hydrogen atom in a molecule of a compound. Carbon NMR (CNMR) is used to determine the type and number of carbon atoms in a given compound (de Paulo *et al.*, 2022).

Magnetic resonance imaging (MRI) is a powerful non-invasive imaging technique that can be employed to produce extremely fine slice-by-slice images of internal structures of various materials using radio waves, a computer, and a strong magnetic field (Awojoyogbe *et al.,* 2016). MRI is used in scientific research and medical diagnosis. Nevertheless, there are limitations associated with MRI. One of the main drawbacks is the high cost of purchasing and

* Corresponding author. Tel.: +2347065698273
E-mail addresses: lateefrasheed01@gmail.com (Rasheed A. Lateef.)

https://doi.org/10.62054/ijdm/0104.12

maintaining an MRI machine. The cost of an MRI machine is typically in the range of hundreds of thousands to millions of dollars, which makes it unaffordable for many individual researchers. In addition, magnetic resonance imaging cannot provide high resolution images of dynamic processes (Zou *et al.,* 2023). NMR is governed by an equation called Bloch NMR fluid flow equation. This is an equation which can be used to define the magnetization of a material such as human blood in terms of blood flow parameters, static magnetic field, time-varying magnetic field and gyromagnetic ratio (Munuera-Javaloy *et al*., 2022).

Previously, many studies have been seen conducted on nuclear magnetic resonance, Bloch NMR equations and their applications (Awojoyogbe *et al.,* 2016; Dada & Awojoyogbe, 2021; Dada *et al.,* 2015; Dubey *et al.,* 2022; Eli & Gyuk, 2015; Emetere, 2013; Hazra *et al.*, 2018; Singh, 2017; Yusuf *et al.,* 2016).

Yusu *et al.* (2024) investigated the effects of relaxation times derived from the Bloch equations on age-related changes in white and grey matter. The findings of the study showed that relaxation times increase with age, reflecting significant alterations in brain tissue, specifically in the degeneration of white matter. Their results provided information about how MRI may be used to investigate brain aging. Firmin *et al.* (1996) investigated the use of magnetic resonance imaging (MRI) in blood flow research, focusing on its potential to give non-invasive and detailed measurements of blood flow dynamics. Their results showed that magnetic resonance imaging (MRI) might be a useful tool for measuring blood flow parameters, such as velocity and relaxation times with great accuracy, providing a number of benefits over convectional techniques. Roche (2004) conducted the assessment of cerebral blood volume as an indicator of angiogenesis induced by chronic hypoxia using steady-state NMR imaging. The purpose of the study was to investigate the relationship between prolonged oxygen deprivation and the formation of new blood vessels in the brain. The results of the study showed that increased blood volume associated with hypoxia-induced angiogenesis could be successfully identified by NMR imaging, providing important new information on vascular changes in the brain and possible diagnosis uses for disorders associated with prolonged oxygen deprivation. Hernandez-Garcia *et al.* (2007) studied the impact of magnetization transfer on the efficiency of flow-driven adiabatic fast passage inversion in arterial blood. The findings of the study showed that the effectiveness of flow-driven inversion is strongly affected by magnetization transfer, highlighting the importance of taking these factors into consideration to increase the accuracy of MRI-based blood flow measurement. Russell (2014) investigated the effect of diffusion and relaxation in magnetic resonance imaging (MRI) using computational modeling. The results of the study indicated that computational modeling can accurately forecast the impact of relaxation and diffusion on MRI results. These results would enhance imaging diagnostics. Odoh and De (2009) investigated the use of nuclear magnetic resonance imaging for estimating blood flow. The aim of this study was to improve non-invasive techniques that could be utilized to measure blood flow rates within the human body. Wright (1991) examined the relaxation behavior of blood under varying magnetic resonance conditions. The study specifically investigated the relaxation properties of blood, which are known to be affected by various factors such as blood flow, hematocrit, and hemoglobin concentration. The findings of the study showed significant new insights into the relaxation behavior of blood, and may lead to enhancements in MRI technique for more accurate imaging and diagnosis of blood-related conditions and vascular health.

Recently, De (2018) and Awojoyogbe *et al.* (2011) derived a single NMR fluid flow equation called Bloch NMR fluid flow equation from a set of three Bloch NMR equations. It was observed that some NMR parameters such as Larmor frequency and static magnetic field of spinning blood protons are absent from their own derivation. Thus, after observing existing work done on nuclear magnetic resonance and Bloch NMR fluid flow equation, we believed that there is still room for further improvement of the Bloch NMR fluid flow equation in such a way that the equation will encompasses amplitude of static magnetic field and Larmor frequency of proton spins. To fill this gap in the existing studies, this study derived a new Bloch NMR fluid flow equation which contains all the NMR parameters. The study also investigated the effect of transverse relaxation times of arterial, venous and capillary blood on magnetization of blood proton spins flowing along the human blood vessels.

1.1 Derivation of Improved Bloch NMR Fluid Flow Equation

During a nuclear magnetic resonance experiment, firstly static magnetic field $\vec{B}_0$ is applied to a spinning nucleus of a given NMR active sample. This static magnetic field is applied to the sample along the z-direction. Secondly, time-varying magnetic field $\vec{B}_1$ is applied to the sample. The vector field $\vec{B}_1$ oscillates in the transverse plane with a frequency ω at time t. Thus, the field $\vec{B}_1$ can be resolved into two components in order to get the relation given as follow:

$$\vec{B}_1 = \hat{i} B_1 \cos\omega t - \hat{j} B_1 \sin \omega t \tag{1}$$

The negative sign in Eq. (1) implies that the field $\vec{B}_1$ rotates in the same direction as that of the precession of nuclear spins.

The total magnetic field $\vec{B}$ which is applied to the NMR active spinning nucleus is the given by the relation:

$$\vec{B} = \hat{i} B_1 \cos\omega t - \hat{j} B_1 \sin \omega t + \hat{k} B_0 \tag{2}$$

where ω is the frequency of precession of the time-varying magnetic field, B_0 is the amplitude of the static magnetic field, B_1 is the amplitude of the time-varying magnetic field.

The torque $\vec{\tau}$ due to the total field $\vec{B}$ acting on a spinning nucleus which has a magnetic moment $\vec{\mu}$ is given by the relation:

$$\vec{\tau} = \vec{\mu} \times \vec{B} \tag{3}$$

According to Newton's second law of rotational motion from classical mechanics, torque $\vec{\tau}$ is the time rate of change of angular momentum, $\vec{L}$ of the spinning nucleus. Then, we have:

$$\vec{\tau} = \frac{d\vec{L}}{dt} \tag{4}$$

The angular momentum, $\vec{L}$ of the spinning nucleus is given by the relation:

$$\vec{L} = \hbar \vec{I} \tag{5}$$

where $\vec{I}$ is the spin of the NMR active nucleus and $\hbar$ is the reduced Planck's constant.
Plugging Eq. (5) into Eqn. (4).Thus, one gets:

$$\frac{d\vec{\mu}}{dt} = \gamma\left(\vec{\mu} \times \vec{B}\right) \tag{6}$$

where

$$\vec{\mu} = \hbar\gamma \vec{I} \tag{7}$$

Considering many nuclei. Thus, Eqn. (6) becomes:

$$\frac{d}{dt}\sum_{i=1}\vec{\mu}_i = \gamma\left(\sum_{i=1}\vec{\mu}_i \times \vec{B}\right) \tag{8}$$

where γ is the gyromagnetic ratio of human blood spinning nuclei.
According to the theory of nuclear magnetic resonance (NMR), magnetization is the sum of the magnetic moments of spinning nuclei present in a given NMR sample. Thus, one gets:

$$\vec{M} = \sum_{i=1}\vec{\mu}_i \tag{9}$$

Putting Eq. (9) into Eq. (8). Thus, one gets:

$$\frac{d\vec{M}}{dt} = \gamma\left(\vec{M} \times \vec{B}\right) \tag{10}$$

Considering the effects of excitation and relaxation. Thus, Eq. (10) becomes:

$$\frac{d\vec{M}}{dt} = \gamma\left(\vec{M}\times\vec{B}\right) - \left(\frac{M_x\hat{i} + M_y\hat{j}}{T_2}\right) - \left(\frac{M_Z - M_0}{T_1}\right)\hat{k} \tag{11}$$

where T_1 is the longitudinal relaxation time of human blood spinning nuclei and T_2 is the transverse relaxation time of human blood spinning nuclei

The first term of Eq. (11) indicates precession and radiofrequency (rf) excitation. These are the change in the direction of magnetization but not the magnitude. The second and third terms of Eq. (11) represent transverse and longitudinal relaxations. These change the magnitude of the magnetization only, not the direction. The magnetization of the nuclei can also be defined by the relation:

$$\vec{M} = M_x\hat{i} + M_y\hat{j} + M_z\hat{k} \tag{12}$$

Using theory of vector calculus and linear operator in Eq. (11). Thus, we get:

$$\begin{aligned} &v^3T_1T_2^2\frac{\partial^3M_y}{\partial x^3} + T_1T_2^2\frac{\partial^3M_y}{\partial t^3} + 3v^2T_1T_2^2\frac{\partial^3M_y}{\partial t\partial x^2} + 3vT_1T_2^2\frac{\partial^3M_y}{\partial x\partial t^2} + \left(2v^2T_1T_2 + v^2T_2^2\right)\frac{\partial^2M_y}{\partial x^2} + \left(T_2^2 + 2T_1T_2\right)\frac{\partial^2M_y}{\partial t^2} \\ &+ \left(4vT_1T_2 + 2vT_2^2\right)\frac{\partial^2M_y}{\partial x\partial t} + \left(T_1 + 2T_2\right)\frac{\partial M_y}{\partial t} + \left(2vT_2 + 2vT_1\right)\frac{\partial M_y}{\partial x} + \left(T_1T_2\gamma^2B_1^2 + \gamma^2T_2^2B_0^2 + 1\right)M_y \\ &= \gamma T_2B_1M_0\cos\omega t - 2T_2^2\gamma^2M_0B_0B_1\sin\omega t \end{aligned} \tag{13}$$

where M_y is the transverse magnetization of human blood spinning nuclei, v is the blood flow velocity, B_0 is the static magnetic field, B_1 is the radio frequency magnetic field, γ is the gyromagnetic ratio of human blood spinning nuclei, ω is the Larmor frequency of spinning nuclei and M_0 is the equilibrium magnetization of human blood.

Equation (13) is the newly developed fluid flow magnetization equation in this study; this is called improved Bloch NMR fluid flow equation. This equation describes the magnetization of spinning nuclei of a given NMR sample such as human blood.

1.2 Dimensional Consistency of Improved Bloch NMR Fluid Flow Equation

In Physics, the method of dimensional analysis can be employed to check the correctness of a derived equation. In order to check the consistency of a given derived equation, one can use the principle of dimensional homogeneity (PDH). Thus, in this study, we utilized the principle of dimensional homogeneity to check the correctness of our newly developed equation given by Eq. (13). This can be achieved as follows:

On taking the dimensions of the both sides of Eq. (13). Thus, one gets:

$$\begin{aligned} &\left[v^3T_1T_2^2\frac{\partial^3M_y}{\partial x^3}\right] + \left[T_1T_2^2\frac{\partial^3M_y}{\partial t^3}\right] + \left[3v^2T_1T_2^2\frac{\partial^3M_y}{\partial t\partial x^2}\right] + \left[3vT_1T_2^2\frac{\partial^3M_y}{\partial x\partial t^2}\right] + \left[\left(2v^2T_1T_2 + v^2T_2^2\right)\frac{\partial^2M_y}{\partial x^2}\right] \\ &+ \left[\left(T_2^2 + 2T_1T_2\right)\frac{\partial^2M_y}{\partial t^2}\right] + \left[\left(4vT_1T_2 + 2vT_2^2\right)\frac{\partial^2M_y}{\partial x\partial t}\right] + \left[\left(T_1 + 2T_2\right)\frac{\partial M_y}{\partial t}\right] + \left[\left(vT_1 + 2vT_2\right)\frac{\partial M_y}{\partial x}\right] \\ &\left[\left(T_1T_2B_1^2\gamma^2 + T_2^2B_0^2\gamma^2 + 1\right)M_y\right] = \left[T_2B_1\gamma M_0\cos\omega t\right] - \left[2\gamma^2M_0T_2^2B_0B_1\sin\omega t\right] \end{aligned} \tag{14}$$

The dimensional formulas for the first and the second terms of Eq. (14) are given as follows:

$$\left[v^3T_1T_2^2\frac{\partial^3M_y}{\partial x^3}\right] = \left[T_1T_2^2\frac{\partial^3M_y}{\partial t^3}\right] = L^{-1}A \tag{15}$$

The dimensional formulas for the third and fourth terms of Eq. (14) are given by the relation:

$$\left[3v^2T_1T_2^2\frac{\partial^3M_y}{\partial t\partial x^2}\right]=\left[3vT_1T_2^2\frac{\partial^3M_y}{\partial x\partial t^2}\right]=3L^{-1}A \tag{16}$$

The dimensional formulas for the fifth and sixth terms of Eq. (14) are defined by the relation:

$$\left[\left(2v^2T_1T_2+v^2T_2\right)\frac{\partial^2M_y}{\partial x^2}\right]=\left[\left(2T_1T_2+T_2^2\right)\frac{\partial^2M_y}{\partial t^2}\right]=3L^{-1}A \tag{17}$$

The seventh term of Eq. (14) is given by the relation:

$$\left[\left(4vT_1T_2+2vT_2^2\right)\frac{\partial^2M_y}{\partial x\partial t}\right]=6L^{-1}A \tag{18}$$

The eighth and ninth terms of Eq. (14) are given as follows:

$$\left[\left(T_1+2T_2\right)\frac{\partial M_y}{\partial t}\right]=\left[\left(vT_1+2vT_2\right)\frac{\partial M_y}{\partial x}\right]=3L^{-1}A \tag{19}$$

The tenth term of Eq. (14) is given as by the relation:

$$\left[\left(T_1T_2\gamma^2B_1^2+T_2^2\gamma^2B_0^2+1\right)M_y\right]=3L^{-1}A \tag{20}$$

The eleventh term of Eq. (14) is given by the relation:

$$\left[T_2\gamma B_1M_0\cos\omega t\right]=L^{-1}A \tag{21}$$

Finally the twelfth term of Eq. (14) is given by the relation:

$$\left[2\gamma^2M_0T_2^2B_0B_1\sin\omega t\right]=2L^{-1}A \tag{22}$$

Plugging Eqs. (15) to (22) into Eq. (14). One gets:

$$29L^{-1}A=L^{-1}A \tag{23}$$

The coefficients at the left hand and right hand sides of Eq. (23) are dimensionless constants. Thus, this makes Eq. (23) to become:

$$L^{-1}A=L^{-1}A \tag{24}$$

Since the right hand side and the left hand side of Eq. (24) are equal. Hence, this means that the newly derived Bloch NMR fluid flow equation given by Eq. (13) in this study is correct.

1.3 Steady State Solution of Improved Bloch NMR Fluid Flow Equation using Laplace Transform Method

In Nuclear Magnetic Resonance (NMR), steady state can be defined as the state in which the magnetization of human blood spinning protons does not change with time. Thus, when blood is flowing steadily along the human blood vessel, all the partial derivatives of the transverse magnetization, M_y with respect to variable t can be set to zero. This makes the third order partial differential equation (13) to reduce to ordinary differential equation whose variable is x. Thus, Eq. (13) becomes:

$$v^3T_1T_2^2\frac{d^3M_y}{dx^3}+\left(2v^2T_1T_2+v^2T_2^2\right)\frac{d^2M_y}{dx^2}+\left(vT_1+2vT_2\right)\frac{dM_y}{dx}+\left(T_1T_2\gamma^2B_1^2+T_2\gamma^2B_0^2+1\right)M_y=T_2B_1M_0\gamma \tag{25}$$

The derivation of Eq. (25) from Eq. (13) is based on the steady-state condition, where the magnetization of human blood proton spins remains constant with time. This means that the magnetization of human blood proton spins is only dependent on the distance along the human blood vessel and is independent of time. Therefore, the time variable t and all the partial derivatives with respect to variable t can be set to zero in Eq. (13). Thus, this leads to the derivation of Eq. (25).

On dividing both sides of Eq. (25) by $v^3T_1T_2^2$, we have:

$$\frac{d^3M_y}{dx^3}+\left(\frac{2T_1+T_2}{vT_1T_2}\right)\frac{d^2M_y}{dx^2}+\left(\frac{T_1+2T_2}{v^2T_1T_2^2}\right)\frac{dM_y}{dx}+\left(\frac{T_1T_2B_1^2\gamma^2+T_2^2B_0^2\gamma^2+1}{v^3T_1T_2^2}\right)M_y=\frac{\gamma B_1M_0}{v^3T_1T_2} \tag{26}$$

Let

$$a_1 = \frac{2T_1 + T_2}{vT_1T_2} \tag{27}$$

$$b_1 = \frac{T_1 + 2T_2}{v^2T_1T_2^2} \tag{28}$$

$$c_1 = \frac{T_1T_2\gamma^2B_1^2 + T_2^2\gamma^2B_0^2 + 1}{v^3T_1T_2^2} \tag{29}$$

$$d_1 = \frac{\gamma B_1M_0}{v^3T_1T_2^2} \tag{30}$$

Putting Eqs. (27) to (30) into Eq. (26).Thus, one gets:

$$\frac{d^3M_y}{dx^3} + a_1\frac{d^2M_y}{dx^2} + b_1\frac{dM_y}{dx} + c_1M_y = d_1 \tag{31}$$

Eq (31) is a non-homogeneous linear differential equation of 3rd order. In order to solve this equation, we employed the Laplace transform method. Thus, we obtained the exact solution of Eq. (31) given as follows:

$$M_y(x) = (g_{23}\cos g_5x + g_{24}\sin g_5x)e^{g_4x} + g_{25}e^{p_1x} + g_{22} \tag{32}$$

where the symbols p_1 and g_i (i= 2,…,25) are defined by the relations given as follows:

$$g_2 = \frac{3b_1 - a_1^2}{3} \tag{33}$$

$$g_3 = \frac{2a_1^3 + 27c_1 - 9a_1b_1}{27} \tag{34}$$

$$p_1 = \left[-\frac{g_3}{2} + \sqrt{\frac{g_2}{27} + \frac{g_3}{4}}\right]^{\frac{1}{3}} + \left[-\frac{g_3}{2} - \sqrt{\frac{g_2}{27} + \frac{g_3}{4}}\right]^{\frac{1}{3}} - \frac{a_1}{3} \tag{35}$$

$$g_4 = -\left(\frac{p_1 + a_1}{2}\right) \tag{36}$$

$$g_5 = \frac{\sqrt{3p_1^2 + 2a_1p_1 + 4b_1 - a_1^2}}{2} \tag{37}$$

$$g_6 = M(0)\left[g_4^3 - 3g_4g_5^2\right] + a_1M(0)\left[g_4^2 - g_5^2\right] + g_4\left[g_1 + b_1M(0)\right] + d_1 \tag{38}$$

$$g_7 = M(0)\left[3g_4^2g_5 - g_5^3\right] + 2a_1g_4g_5M(0) + g_5\left[g_1 + b_1M(0)\right] \tag{39}$$

$$g_8 = 2g_5(g_5p_1 - 2g_4g_5) \tag{40}$$

$$g_9 = 2g_5\left(g_4^2 - g_4p_1 - g_5^2\right) \tag{41}$$

$$g_{10} = \frac{g_6 g_8 + g_7 g_9}{g_8^2 + g_9^2} \tag{42}$$

$$g_{11} = \frac{g_7 g_8 - g_6 g_9}{g_8^2 + g_9^2} \tag{43}$$

$$g_{12} = \frac{g_8}{g_8^2 + g_9^2} \tag{44}$$

$$g_{13} = \frac{g_9}{g_8^2 + g_9^2} \tag{45}$$

$$g_{14} = M(0)\left[g_4^3 - 3g_4 g_5^2\right] + a_1 M(0)\left[g_4^2 - g_5^2\right] + g_4 b_1 M(0) + d_1 \tag{46}$$

$$g_{15} = M(0)\left[3g_4^2 g_5 - g_5^3\right] + 2a_1 g_4 g_5 M(0) + g_5 b_1 M(0) \tag{47}$$

$$g_{16} = g_{12} g_{14} + g_{13} g_{15} \tag{48}$$

$$g_{17} = g_{12} g_4 + g_{13} g_5 \tag{49}$$

$$g_{18} = g_{12} g_{15} - g_{13} g_{14} \tag{50}$$

$$g_{19} = g_{12} g_5 - g_{13} g_4 \tag{51}$$

$$g_{20} = \frac{p_1}{3p_1^3 + 2a_1 p_1^2 + b_1 p_1} \tag{52}$$

$$g_{21} = \frac{M(0)p_1^3 + a_1 M(0)p_1^2 + b_1 p_1 M(0) + d_1}{3p_1^3 + 2a_1 p_1^2 + b_1 p_1} \tag{53}$$

$$g_{22} = \frac{d_1}{c_1} \tag{54}$$

$$g_{23} = 2g_{16} + 2g_1 g_{17} \tag{55}$$

$$g_{24} = -\left(2g_{18} + 2g_1 g_{19}\right) \tag{56}$$

$$g_{25} = g_1 g_{20} + g_{21} \tag{57}$$

2. Materials and Methods

2.1 Materials

The materials used in this study for data analysis and simulations are MATLAB and Origin software tools. MATLAB was used to generate data from steady state solution defined by Eq. (32). Origin software tool was used to plot graphs which were used to visually represent the computational data that was generated in this study for

simulations.

2.2 Methods

Laplace transform method was used for this study to obtain the closed form solution of the improved Bloch NMR fluid flow equation given by Eq. (13) at steady state.

2.3 NMR Blood Flow Constants and Parameters used for Simulations

The steady state solution given by Eq. (32) of the improved Bloch NMR fluid flow Eq. (13) depends on NMR blood flow constants and parameters. Thus, in order to simulate the effect of blood flow parameters, transverse relaxation times of venous, arterial and capillary blood samples on the magnetization distribution of human blood spins; we used the values of the blood flow constants and parameters shown in Tables 1 and 2.

Table 1: Blood Flow Constants used for Simulations

Blood Flow Constant	Value
Blood flow velocity (v)	$0.2m/s$
Gyromagnetic ratio (γ)	$2.6752\times10^{8}rads^{-1}T^{-1}$
Equilibrium Magnetization (M_0)	$1A/m$
Length of human blood vessel (L)	$0.2m$
Longitudinal relaxation time (T_1) for arterial human blood sample	$1516ms$
Longitudinal relaxation time (T_1) for venous human blood sample	$1547ms$
Longitudinal relaxation time (T_1) for capillary human blood sample	$300ms$
Human blood vessel right hand side boundary condition [$M(0)$]	$1A/m$
Human blood vessel left hand side boundary condition [$M(L)$]	$0\ A/m$
Radio frequency magnetic field (B_1)	$1G$
Static magnetic field(B_0)	$1.5T$

Table 2: Blood Flow Parameters used for Simulations

Blood Flow Parameter	Value

Transverse relaxation time (T_2) for arterial human blood sample	(228-280)ms
Transverse relaxation time (T_2) for venous human blood sample	(158-204)ms
Transverse relaxation time (T_2) for capillary human blood sample	(10-200)ms

3. Results and Discussion

3.1 Results

3.1.1 Results of Effect of Transverse Relaxation Times on Magnetization of Spinning Protons of Arterial Blood at Steady State

The results of the effect of the blood flow parameter, transverse relaxation times on the magnetization of arterial blood spinning protons at steady state defined by Eq. (32) are shown in figures 3.1 (a-d). These results show the variation in magnetization of spinning protons in arterial blood as a function of distance along the human blood vessel at $T_1 = 1387ms$ for arterial blood flow parameter values $T_2 = 228ms$, $245ms$, $262ms$, and $279ms$.

3.1.2 Results of Effect of Transverse Relaxation Times on Magnetization of Spinning Protons of Venous Blood at Steady State

The results of the effect of the blood flow parameter, transverse relaxation times on the magnetization of venous blood spinning protons at steady state defined by Eq. (32) are shown in figures 3.2 (e-h). These results show the variation in magnetization of spinning protons in venous blood as a function of distance along the human blood vessel for venous blood flow parameters $T_2 = 158ms$, $173ms$, $188ms$, and $203ms$ at $T_1 = 1381ms$.

3.1.3 Results of Effect of Transverse Relaxation Times on Magnetization of Spinning Protons of Capillary Blood at Steady State

The results of the effect of the blood flow parameter, transverse relaxation times on the magnetization of capillary blood spinning protons at steady state defined by Eq. (32) are shown in figures 3.3 (i-l). These results show the variation in magnetization of spinning protons in capillary blood as a function of distance along the human blood vessel for capillary blood flow parameters $T_2 = 10ms$, $73ms$, $136ms$, and $199ms$ at $T_1 = 300ms$.

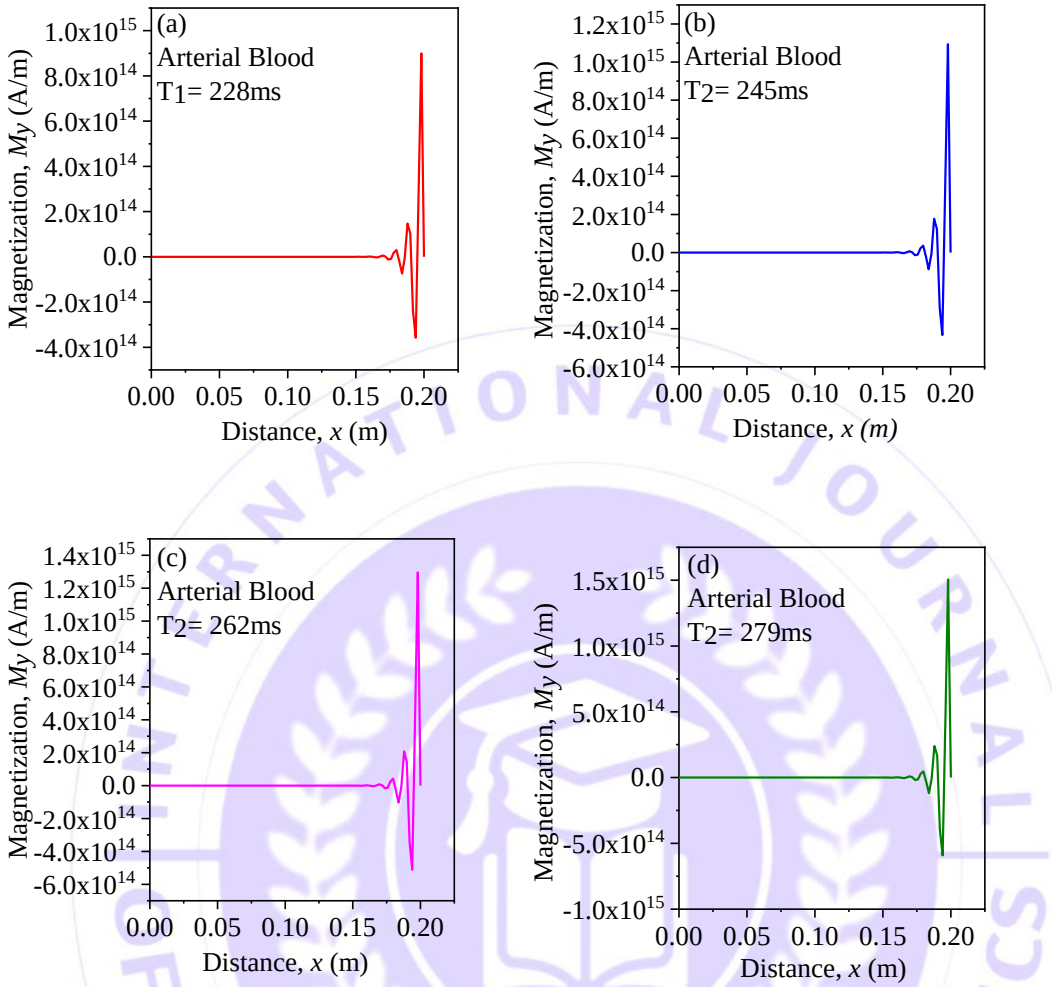

Figure. 1: 2D plots of magnetization of the human blood proton spins as a function of distance along the blood vessel for arterial blood with (a) T_2=228ms (b) T_2=245ms (c) T_2=262ms (d) T_2=279ms. These plots were obtained from steady state solution 32 of equation 13.

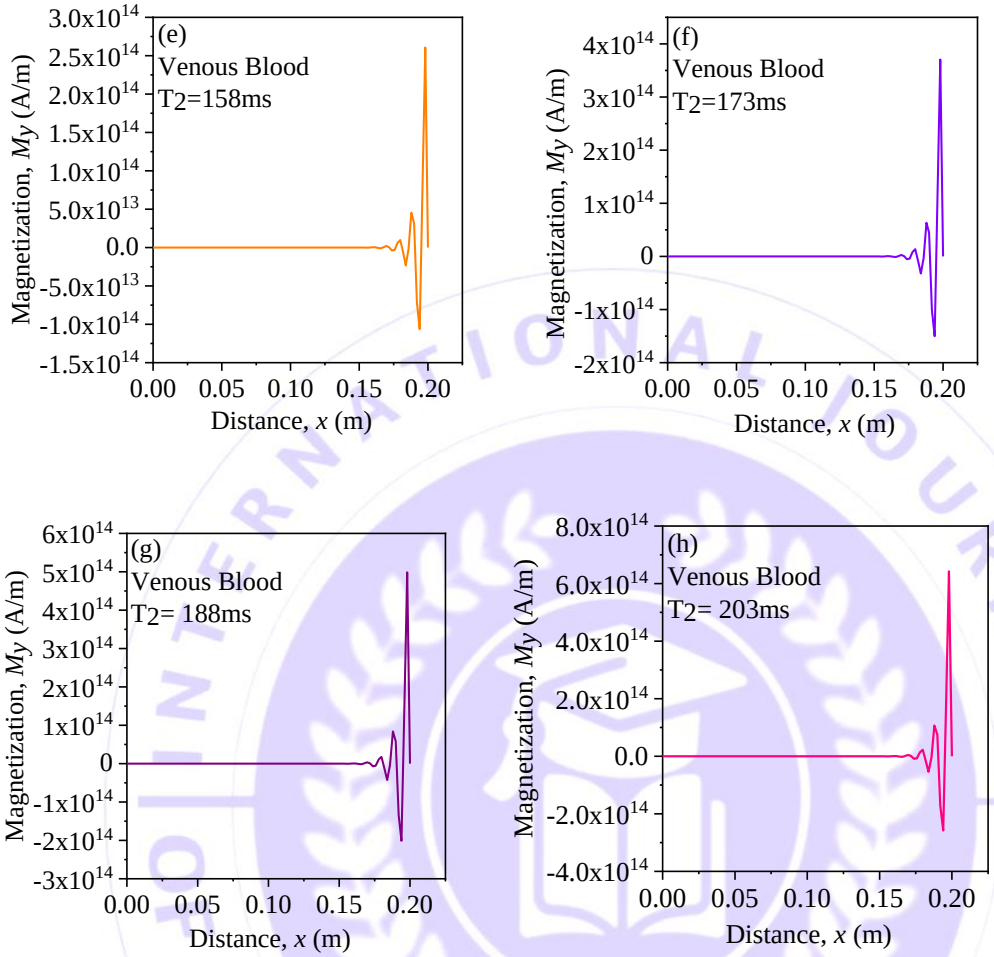

Figure 2: 2D plots of magnetization of the human blood proton spins as a function of distance along the blood vessel for venous blood with (e) T_2=158ms (f) T_2=173ms (g) T_2=188ms (h) T_2 =203ms. These plots were generated from steady state solution 32 of equation 13.

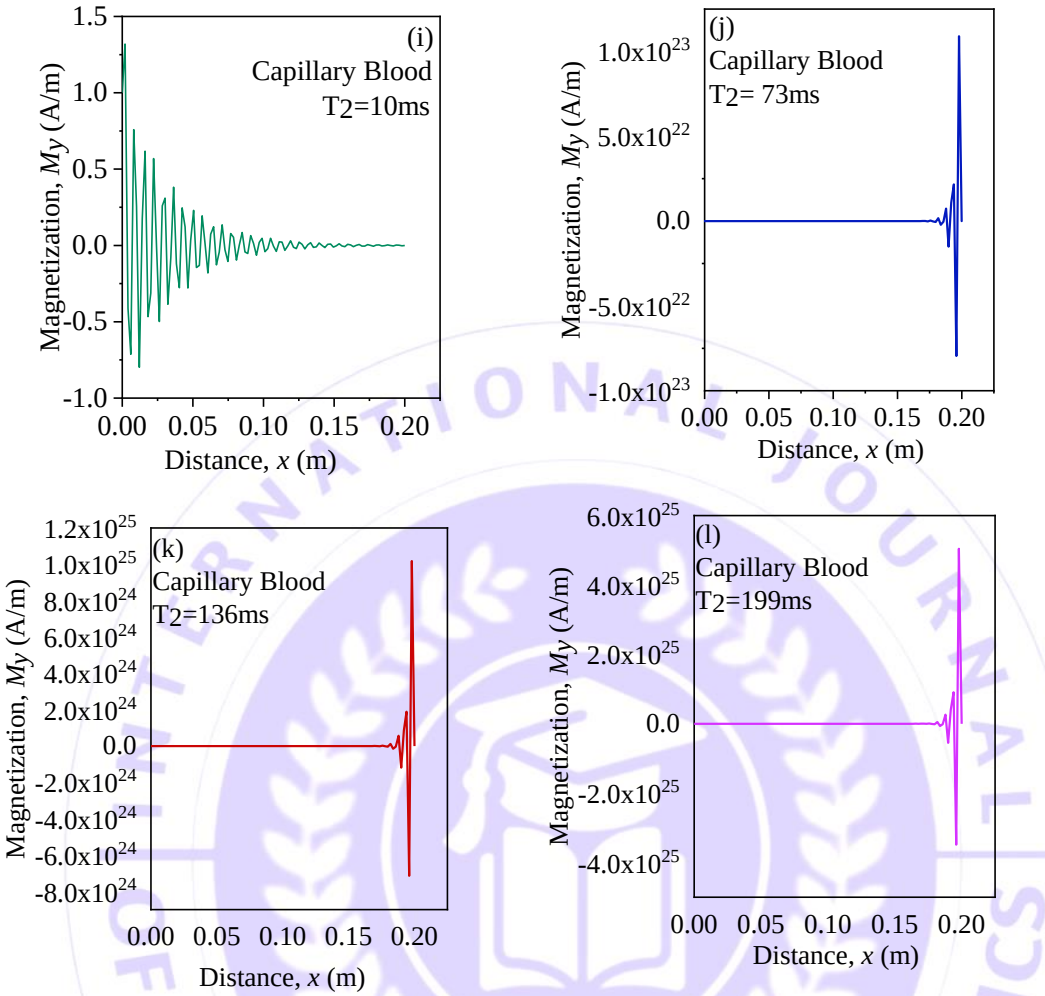

Figure 3: 2D plots of magnetization of the human blood proton spins as a function of distance along the blood vessel for capillary blood with (i) T_2=10ms (j) T_2=73ms (k) T_2=136ms (l) T_2=199ms. These plots were generated from steady state solution 32 of equation 1.

3.2 Discussion

The results obtained in figures 3 (a-l) depict the variation of magnetization distribution of human blood proton spins with distance along the human blood vessel for various transverse relaxation time of venous, arterial and capillary blood samples respectively. The figures show that magnetization distribution of spinning blood protons contains two components: the linear and the non-linear components. Thus, the linear component implies that for varied relaxation times of venous, arterial and capillary blood respectively, the magnetization of blood proton spins remains constant as blood proton spins flow along the human blood vessels. The non-linear component implies that for varied transverse relaxation times of venous, arterial and capillary blood respectively, the magnetization of human blood proton spins changes as blood proton spins flow along the human blood vessels. The results also showed that capillary blood proton spins undergo phase coherence, which means that they move in step.

4 Conclusion

In this study, we have derived a novel Bloch NMR flow equation, which is called the improved Bloch NMR fluid flow equation, and also obtained its steady-state solution. Furthermore, we investigated the effect of relaxation times of arterial, venous and capillary blood on magnetization of spinning blood protons at steady state. The results of the study showed that for varied relaxation times of venous, arterial and capillary blood, respectively, the magnetization of human blood proton spins initially remain constant and then changes as blood proton spins flow along the human blood vessels. The findings of the study also revealed that the proton spins of blood flowing through human capillaries exhibit phase coherence.

References

Awojoyogbe, B. O., Dada, M. O., Onwu, S. O., Ige, T. A., & Akinwande, N. I. (2016). Computational diffusion magnetic resonance imaging based on time-dependent Bloch NMR flow equation and Bessel functions. *Journal of Medical Systems*, *40*(4), Article 4.

Awojoyogbe, O. B., Dada, O. M., Faromika, O. P., & Dada, O. E. (2011). Mathematical concept of the Bloch flow equations for general magnetic resonance imaging: A review. *Concepts in Magnetic Resonance Part A*, *38A*(3), 85–101.

Dada, M. O., & Awojoyogbe, B. O. (2021). Analysis of the Hydrogen-Like Atom for Neuro- Oncology Based on Bloch's NMR Flow Equation. In *Computational Molecular Magnetic Resonance Imaging for Neuro-oncology* (pp. 219–246). Springer.

Dada, O. M., Awojoyogbe, O. B., & Ukoha, A. C. (2015). A computational analysis for quantitative evaluation of petrol-physical properties of rock fluids based on Bloch NMR diffusion model for porous media. *Journal of Petroleum Science and Engineering*, *127*, 137–147.

De, D. K. (2018). New Formulation of Magnetization Equation for Flowing Nuclear Spin Under Nuclear Magnetic Resonance/Magnetic Resonance Imaging Excitation. *Journal of Engineering and Science in Medical Diagnostics and Therapy*, *1*(2), Article 2.

de Paulo, E. H., dos Santos, F. D., Folli, G. S., Santos, L. P., Nascimento, M. H., Moro, M. K., da Cunha, P. H., Castro, E. V., Neto, A. C., & Filgueiras, P. R. (2022). Determination of gross calorific value in crude oil by variable selection methods applied to 13C NMR spectroscopy. *Fuel*, *311*, 122527.

Dubey, V. P., Singh, J., Alshehri, A. M., Dubey, S., & Kumar, D. (2022). Forecasting the behavior of fractional order Bloch equations appearing in NMR flow via a hybrid computational technique. *Chaos, Solitons & Fractals*, *164*, 112691.

Eli, D., & Gyuk, P. M. (2015). Analytical solution to diffusion-advection equation in spherical coordinate based on the fundamental Bloch NMR flow equations. *Int. J. Theor. Math. Phys*, *5*(5), Article 5.

Emetere, M. (2013). Mathematical modelling of Bloch NMR to explain the Rashba Energy Features. *World Journal of Condensed Matter Physics*, *3*, 87–94.

Firmin, D. N., Mohiaddin, R. H., & Filling, G. V. (1996). The Application of Magnetic Resonance to Blood Flow Studies. *Advances in Hemodynamics and Hemorheology, Volume 1*, *1*, 145.

Gao, S., Xu, J., & Lu, W. (2019). Research on the improvement of the diagnostic effect of machine learning on nuclear magnetic resonance of brain tumors. *Journal of Intelligent & Fuzzy Systems*, *37*(5), Article 5.

Hazra, A., Lube, G., & Raumer, H. G. (2018). Numerical simulation of Bloch equations for dynamic magnetic resonance imaging. *Applied Numerical Mathematics*, *123*, 241–255.

Hernandez-Garcia, L., Lewis, D. P., Moffat, B., & Branch, C. A. (2007). Magnetization transfer effects on the efficiency of flow-driven adiabatic fast passage inversion of arterial blood. *NMR in Biomedicine: An International Journal Devoted to the Development and Application of Magnetic Resonance In Vivo*, *20*(8), 733–742.

Munuera-Javaloy, C., Tobalina, A., & Casanova, J. (2022). High-Resolution NMR Spectroscopy at Large Fields with Nitrogen Vacancy Centers. *arXiv Preprint arXiv:2205.04150*.

Odoh, E. O., & De, D. K. (2009). Analytical Solutions of NMR Bloch Equations for Human Blood Flow by Laplace Transform. *J. Inst. Math. Comput. Sci.(India).*, *22*(2), Article 2.

Rasheed, L., & Usman, A. (2023). Analytical solution of Bloch NMR fluid flow space–time-dependent equation using Laplace transform and complex inversion integral. *International Journal of Modern Physics B*, 2450052.

Roche, M. A. (2004). *Steady state NMR imaging of cerebral blood volume as an index of chronic hypoxia induced angiogenesis*. Dartmouth College.

Russell, G. (2014). *Understanding the Effects of Diffusion and Relaxation in Magnetic Resonance Imaging using Computational Modeling*.

Singh, D. V. (2017). *Role of Multidetector Computed Tomography in Pulmonary Arterial Disease.* [PhD Thesis].

Singh, H. (2017). Operational matrix approach for approximate solution of fractional model of Bloch equation. *Journal of King Saud University-Science*, *29*(2), Article 2.

Strogatz, S. H. (2018). *Nonlinear dynamics and chaos: With applications to physics, biology, chemistry, and engineering*. CRC press.

Turkbey, B., Mani, H., Shah, V., Rastinehad, A. R., Bernardo, M., Pohida, T., Pang, Y., Daar, D., Benjamin, C., & McKinney, Y. L. (2011). Multiparametric 3T prostate magnetic resonance imaging to detect cancer: Histopathological correlation using prostatectomy specimens processed in customized magnetic resonance imaging based molds. *The Journal of Urology*, *186*(5), Article 5.

Wright, G. A. (1991). *Magnetic resonance relaxation behavior of blood: Study and applications*. Stanford University.

Yusu, S. I., Olaoye, D. O., Dada, M. O., Saba, A., Audu, K. J., Ibrahim, J. A., & Jatto, A. O. (2024). Effects of Relaxation Times from the Bloch Equations on Age Related Changes in White and Grey Matter. *International Journal of Mathematical Sciences and Optimization: Theory and Applications*, *10*(1), 93–105.

Yusuf, S. I., Aiyesimi, Y. M., Jiya, M., & Awojoyogbe, O. B. (2016). *Analytical Solution of the Bloch NMR Flow Equations for the Analysis of Blockage in a Radially Symmetric Cylindrical Pipe*.

Zou, B., Ji, Z., Zhu, C., Dai, Y., Zhang, W., & Kui, X. (2023). Multi-scale deformable transformer for multi-contrast knee MRI super-resolution. *Biomedical Signal Processing and Control*, *79*, 104154.